


L. V. Batyuk

PhD biol, docent

Assoc. Prof. Dep. of Med. Biol. Phys. and Med. Inform.

Kharkiv National Medical University

4 Nauki av., Kharkiv, Ukraine, 61000

lili.batyuk@gmail.com  <http://orcid.org/0000-0003-1863-0265>


N. M. Kizilova

DSc mech, prof.

Prof. Dep. Appl. Math.

V. N. Karazin Kharkiv National University

4 Svobody Sq., Kharkiv, Ukraine, 61022

n.kizilova@gmail.com  <http://orcid.org/0000-0001-9981-7616>


S. O. Poslavski

PhD mech

Assoc. Prof. Dep. Appl. Math.

V. N. Karazin Kharkiv National University

4 Svobody Sq., Kharkiv, Ukraine, 61022

s.poslavski@gmail.com  <http://orcid.org/0000-0002-1049-9947>

A review on rheological models and mathematical problem formulations for blood flows

A review on constitutive equations proposed for mathematical modeling of laminar and turbulent flows of blood as a concentrated suspension of soft particles is given. The rheological models of blood as a uniform Newtonian fluid, non-Newtonian shear-thinning, viscoplastic, viscoelastic, tixotropic and micromorphic fluids are discussed. According to the experimental data presented, the adequate rheological model must describe shear-thinning tixotropic behavior with concentration-dependent viscoelastic properties which are proper to healthy human blood. Those properties can be studied on the corresponding mathematical problem formulations for the blood flows through the tubes or ducts. The corresponding systems of equations and boundary conditions for each of the proposed rheological models are discussed. Exact solutions for steady laminar flows between the parallel plates and through the circular tubes have been obtained and analyzed for the Ostwald, Hershel-Bulkley, and Bingham shear-thinning fluids. The influence of the model parameters on the velocity profiles has been studied for each model. It is shown, certain sets of fluid parameters lead to flattening of the velocity profile while others produce its sharpening around the axis of the

© L. V. Batyuk, N. M. Kizilova, S. O. Poslavsky, 2023

channel. It is shown, the second-order terms in the viscoelastic models give the partial derivative differential equations with high orders in time and mixed space-time derivatives. The corresponding problem formulations for the pulsatile flows of the fluids with generalized rheological laws through the soft tubes are derived. Their analytical solutions for the flow velocity, hydrostatic pressure and cross-sectional area of the tube are derived in the form of the normal mode. It is shown, the dispersion equations produce an additional set for the speed of sound (so called second sound) in the fluid. It is concluded, the most general rheological model of blood must include shear-thinning, concentration and second sound phenomena.

Keywords: differential equations; rheological models; suspensions; fluid dynamics.

2010 Mathematics Subject Classification: 93C20; 76Axx; 35Q35.

1. Introduction

Recent progress in numerical methods and high performance computing stimulated development of sophisticated patient-specific mathematical models for different physiological systems, organs and tissues [1,2]. The models are based on the systems of partial differential equations (PDE) described the blood flow as a viscous liquid (i) along the complex tree-type or network-type structures of the blood vessels (ii) accounting for the complicated rheological relationships for the blood (iii) and viscoelastic walls (iv) of arteries, veins and capillaries. The first set of PDE (i) comprises the compressible Navier-Stokes equations for the hydrostatic pressure p_b , blood flow velocity \vec{v}_b and temperature T_b . Dynamics of the blood vessel walls (ii) which are in direct fluid-structure interaction (FSI) with the blood flow is described based on the 3D models of viscoelastic solid [3], 2D thin wall models [4], shell theory models [5], or membrane models [6] for the vessel walls. The two sets (i), (ii) of PDEs give a formulation of the FSI problem in mathematical hemodynamics [3,4]. Both sets are interconnected via common boundary conditions (BC) at the fluid-solid interfaces. In the case of non-Newtonian models of blood and viscoelastic vessel wall, the systems (i), (ii) are combined via the flow-dependent material parameters (blood viscosity μ_b , wall viscosity μ_w , etc.) and temperature dependencies. The governing system (i)-(ii) accounted for complex rheological relations (iii)-(iv) is quite sensitive to the choice of rheological models and material parameters [3-6]. Therefore, significant attention has been paid to experimental and theoretical study of blood rheology and vessel wall rheology.

The linear relationship between the shear rate $\dot{\gamma}$ and shear stress τ in the moving fluids was first discovered by I. Newton in his experiments with uniform liquids [7]. In 1836-1848 French doctor J. Poiseuille experimentally studied slow steady flows of different fluids (including blood of some experimental animals) through circular glass and copper tubes, and found the linear dependence between the pressure drop Δp from the inlet to the outlet of the tube and the volumetric

flow rate Q (Hagen-Poiseuille law). In 1845 English mathematician G. Stokes published mathematical derivation of the Hagen-Poiseuille formula

$$Q = \frac{\pi R^4 \Delta p}{8\mu_b L}, \tag{1}$$

where R and L are the radius and length of the tube.

Eq.(1) allows experimental estimation of the fluid viscosity when the value Q can be measured at a given $\Delta p = const$. In 1930-th it was shown in a series experiments that the blood flows through small capillaries ($R \leq 100\mu m$) are characterized by lower values of μ_b at low shear rates, while in the larger tubes it is noticeably higher. The effect was discovered by R. Fahraeus and T. Lindqvist [8]. Besides, μ_b increases with shear rate $\dot{\gamma}$ of the flow, and at $\dot{\gamma} \geq 100s^{-1}$ it becomes almost constant (i.e. flow-independent). In order to keep the same general form (1) of the Hagen-Poiseuille law, the efficient viscosity was introduced as

$$\mu_{eff} = k \frac{\Delta p}{Q(\Delta p)}, \quad k = \frac{\pi R^4}{8L}, \tag{2}$$

computed from (1) on the experimental data; the efficient viscosity can be a flow-dependent function $\mu_{eff}(\dot{\gamma})$.

Later the Fahraeus-Lindqvist effect was found not only in blood but also in other suspensions of small solid particles in a uniform fluid. In some suspensions $d\mu_{eff}/d\dot{\gamma} > 0$ (shear-thickening fluids) while in others $d\mu_{eff}/d\dot{\gamma} < 0$ (shear-thinning fluids). For dilute suspensions the effect was explained by the particle-free layer (PFL) appeared near the wall of the tube (Fig.1a) due to the net hydrodynamic forces directed the particles towards the axis of the capillary (Segre–Silberberg effect). One of the main components of the net force is the Magnus force acting on the rotating particles in the Newtonian fluid flow [9,10]. In the flows of diluted blood, the cell-free layer of the thickness $\delta \sim 3\mu m$ composed by the blood plasma (BP) only is clearly visible in the glass tubs, small arteries and capillaries (Fig.1b). The value of δ is comparable to the mean radius of the red blood cells (RBC) $r_{RBC} = 3.5\mu m$.

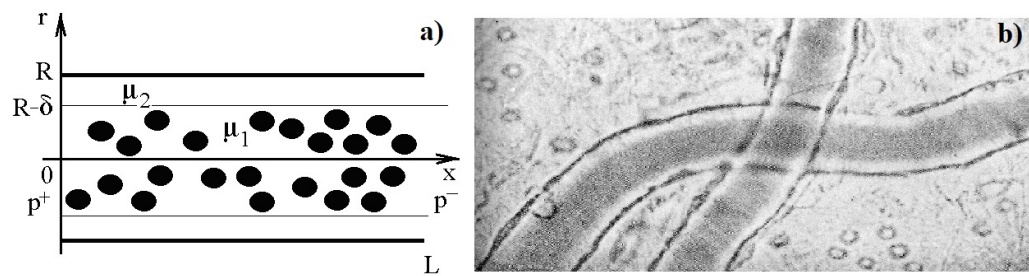


Fig. 1. Cell-free layer in the flows of suspensions: a) a scheme; b) the blood flow with a PFL in a small artery.

The simplest mathematical model of the Fahraeus-Lindqvist effect is based on the Poiseuille flow of two immiscible fluids through a circular tube. The fluids occupy the core of the flow (Fig.1a) $V_{core} = \{r \in [0, R - \delta], x \in [0, L]\}$ and the PFL $V_{PFL} = \{r \in [R - \delta, R], x \in [0, L]\}$ with the viscosities μ_1 and μ_2 , respectively. Solution of the incompressible Navier-Stokes equations (Poiseuille flow) of the two liquids with the velocity and shear stress continuity BC at the interface $r = R - \delta$ gives the following expression for the efficient viscosity [11]

$$\mu_{eff} = \frac{\mu_2}{1 - (1 - \mu_2/\mu_1)(1 - \delta/R)^4}. \quad (3)$$

At $\delta = const$ (3) gives $d\mu_{eff}/dR > 0$ that corresponds to the Fahraeus-Lindqvist effect.

Important contributions to rheology and the theory of fluid flows was done by French physicist M. Couette who experimentally studied (in 1880-th) steady flows between two rotating coaxial cylinders. His rotational rheometer is one of the most popular types of the viscometers used for the viscosity measurements until nowadays. Detailed experiments with blood in the capillary, rotational and other types of viscometers [12-14] revealed some other rheological properties of blood (behind its shear-thinning properties), namely

1) the dependency $\mu_b(C_{RBC})$ on the RBC concentration C_{RBC} (or its medical term hematocrit Ht);

2) thixotropy (time-dependent shear-thinning due to the RBC aggregation/disaggregation);

3) viscoplasticity with the yield stress τ_0 ;

4) viscoelasticity (a combination of viscous and elastic properties);

5) micromorphic properties (due to local flow-induced deformations of RBC).

Some of those properties promote increase in the blood viscosity, while others led to its decrease, and their combination can produce some paradoxical effects like a constant viscosity measured at the presence of two opposed effects [15].

Besides, more rheological effects are produced by specific biochemical nature of the blood as a cellular suspension and its electromagnetic properties [16], namely

6) Electric potential of the RBC surface due to specific distribution of the positive and negative charged molecular groups in the outer layer (glycocalyx) and electric interaction (mostly repulsion) between the cells;

7) Formation of the hydration layer around the RBC in the aqueous solutions (in blood plasma as water solution of mineral and organic components);

8) Copley-Scott Blair phenomenon (specific adsorption of large molecules and cells to the vessel wall that lead to the double electric layer (DEL) formation, electric interaction with the moving cells and ions, and physical decrease in the vessel diameter) [10,17,18];

9) Active movement of leukocytes to/away from a chemokinetic agent [19];

10) Movement of leukocytes out of blood vessels through the vessel wall (extravasation) to the location of tissue damage/inflammation.

More complex effects are connected with the local, humoral and nervous regulation like

- 11) Local release of the chemical factors influencing the cell properties, wall thickness and vessel diameter, and therefore, the blood velocity;
- 12) Movement of the blood cells into the circulatory system from the marrow;
- 13) Release an additional blood volume into the circulation from the spleen;
- 14) Movement of the water component from/into the vessels controlled by the volume receptors in the vessel wall.

In this paper a review of the most popular rheological models of blood is presented, and the corresponding mathematical formulations for the blood flow in the blood vessels, tubes of biomedical units like cardiopulmonary bypass, microfluidic systems, lab-on-a-chip or experimental equipment are discussed.

2. Classification of the rheological models of blood.

2.1. Newtonian fluid model.

Newtonian fluid model has a flow-independent viscosity $\mu_b = \mu_b(T, C_j)$ only dependent on the temperature T and concentrations C_j of some specific components like polyacrylic polyethylene. Small concentrations of those polymers can decrease the blood viscosity that is used in reanimation protocols. They can also decrease the flow resistivity in the high Reynolds regimes (polymer turbulence drag reduction Toms effect). In the simplest cases the Newton fluid approach $\mu_b = const$ can be accepted and then the basic mathematical model of the blood flow is the incompressible Navier-Stokes equations

$$\begin{cases} \operatorname{div}(\vec{v}) = 0, \\ \rho_b \frac{d\vec{v}}{dt} = -\nabla p + \mu_b \Delta \vec{v} + \rho_b \vec{f}, \end{cases} \quad (4)$$

where \vec{f} is the external net force.

This approach is valid for the large vessels ($d > 1 - 5mm$) and high shear rates $\dot{\gamma} > 200 - 400c^{-1}$. In the case of rigid boundaries and steady 1D flow (4) has analytical solutions for a cylindrical tube with any arbitrary smooth cross-sectional perimeter [7]. Such solutions are usually used for validation of the numerical models (finite difference, finite elements, finite volumes and others). The turbulent flows of blood at higher Reynolds numbers $Re=1000-6000$ can also be computed by direct numerical computations on (1); therefore particular turbulent models ($k - \varepsilon$, $k - \omega$, Spalart-Allmaras and others) are not considered here.

2.2. Shear-thinning models.

According to numerous experimental results, blood exhibits shear-thinning properties that can be modeled as a linear dependence between the shear stress τ_{ik} and shear rate v_{ik} tensors with viscosity dependent on the components of the shear rate tensor $\tau_{ik} = 2\mu_b(T, C_j, v_{ik}) v_{ik}$. Since viscosity is a scalar function, the allowed dependence is $\mu_b = \mu_b(I_{1v}, I_{2v}, I_{3v})$, where $I_{1v} = \operatorname{Tr}\{v_{ik}\} = v_{kk}$, $I_{2v} = v_{xx}v_{yy} + v_{yy}v_{zz} + v_{xx}v_{zz} - v_{xy}^2 - v_{yz}^2 - v_{xz}^2$, $I_{3v} = \operatorname{Det}|v_{ik}|$ are the main invariants of

the strain tensor. For an incompressible fluid $I_{1v} = 0$ and the simplest rheological model is $\mu_b = \mu_b(I_{2v})$. When a synthetic invariant $I_v = \sqrt{2(I_{1v}^2 - 2I_{2v})}$ is used instead of I_{2v} , for the 1D flows $I_v = \dot{\gamma}$ that is convenient for both experiments and theoretical considerations. Therefore, the simplest rheological model of the blood as a shear-thinning fluid is $\mu_b = \mu_b(T, C_j, \dot{\gamma})$, where $\partial\mu_b/\partial\dot{\gamma} < 0$. The very first power model was proposed by Ostwald in the form

$$\mu = \tau/\dot{\gamma} = k(\dot{\gamma})^{n-1}, \quad (5)$$

where $0 < n < 1$. The value of n is computed from experiments with blood flows at different shear rates $\dot{\gamma}$.

Substitution of (5) or any other complex rheological law into (4) gives the non-linear system of PDEs

$$\begin{cases} \operatorname{div}(\vec{v}) = 0, \\ \rho_b \frac{d\vec{v}}{dt} = -\nabla p + \mu_b(I_v) \Delta \vec{v} + \rho_b \vec{f}. \end{cases} \quad (6)$$

For instance, for the 1D Poiseuille flow between two parallel plates along the axis $0x$ (5), (6) gives

$$\begin{cases} \frac{\partial v_x}{\partial x} = 0, \\ \frac{\partial p}{\partial x} = \frac{k}{r} \frac{\partial}{\partial r} \left(r \frac{\partial v_x}{\partial r} \right) \left(\frac{\partial v_x}{\partial r} \right)^{n-1} + \rho_b f_x. \end{cases} \quad (7)$$

It is clear, the parabolic Poiseuille or linear Couette flow profiles do not satisfy (7). Its solution can be found by numerical methods. In the case of the circular tube and $f_x = 0$ an analytical solution of (7) with the no-slip boundary conditions (BC) at the walls gives [20]

$$v(r) = \frac{nR}{(n+1)} \left(\frac{R\Delta p}{2kL} \right)^{1/n} \left(1 - \left(\frac{r}{R} \right)^{(n+1)/n} \right). \quad (8)$$

The velocity profiles computed in (8) for different values $n \in]0, 1[$ are flattened (Fig.2a) compared to the parabolic solution (at $n=1$) while for the shear thickening fluids ($n>1$) they become closer to the cone-type profile sharpened around the axis $0r$ (Fig.2b).

2.3. Viscoplastic models.

As other suspensions of aggregating particles, for starting the movement blood needs a big enough shear stress $\tau > \tau_0$, where τ_0 is the yield stress needed to destroy the network of aggregates (Fig.3a) those are chains of the RBCs (Fig.3b) such as

$$\begin{aligned} \dot{\gamma} &= 0 & \text{when } \tau < \tau_0, \\ \dot{\gamma} &> 0 & \text{when } \tau > \tau_0. \end{aligned} \quad (9)$$

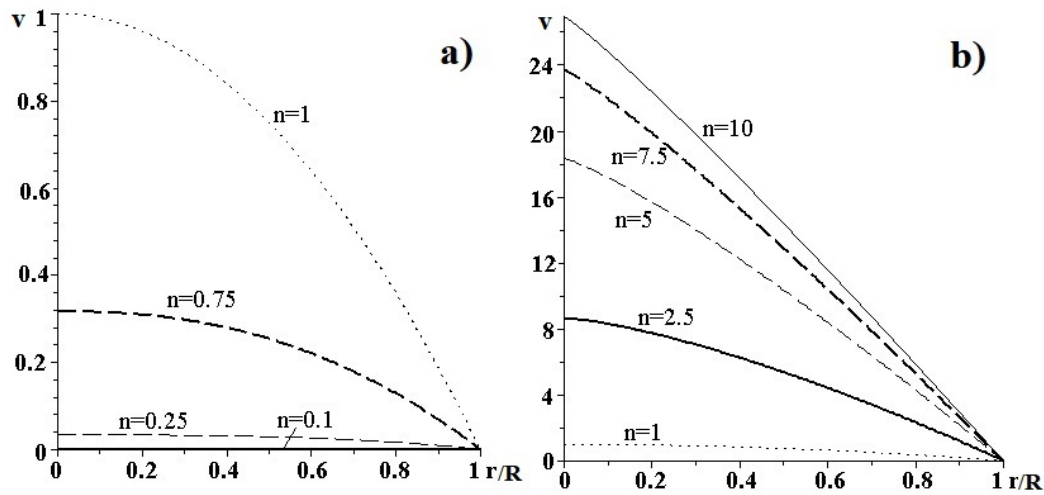


Fig. 2. Velocity profiles $v(r)$ for the Ostwald fluid flow:
 a) at $0 < n < 1$; b) at $n > 1$.

The simplest linear model of (9) was proposed by E.C.Bingham (1916)

$$\tau = \tau_0 + \mu\dot{\gamma}, \quad \text{when } \tau > \tau_0 \tag{10}$$

or in the tensorial form

$$\tau_{ik} = 2 \left(\frac{\tau_0}{I_v} + \mu \right) v_{ik}, \quad \sqrt{I_{2\tau}} > 2\tau_0. \tag{11}$$

where $I_{2\tau}$ is the second invariant of the shear stress tensor τ_{ik} .

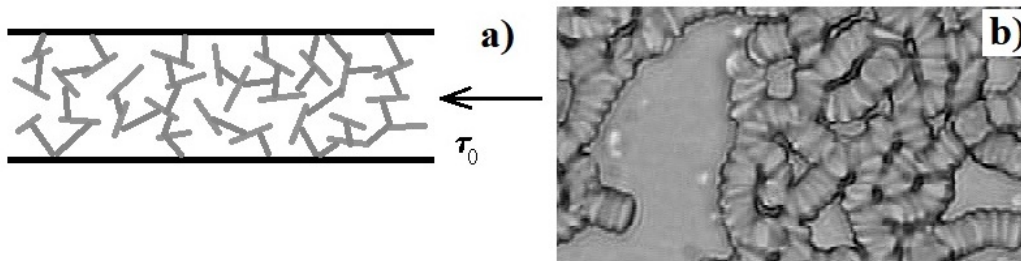


Fig. 3. a) A network of aggregates in the model viscoplastic fluid;
 b) RBC chains in the blood.

A non-linear rheological model was proposed by N. Casson (1959) based on his experiments with pigment-oil suspensions of the ink type [21]

$$\sqrt{\tau} = \sqrt{\tau_0} + \sqrt{\mu_b \dot{\gamma}}, \quad \text{when } \tau > \tau_0 \tag{12}$$

or in the tensorial form

$$\tau_{ik} = 2 \left(\sqrt{\frac{\tau_0}{I_v}} + \sqrt{\mu_b} \right)^2 v_{ik}, \quad \sqrt{I_{2\tau}} > 2\tau_0. \quad (13)$$

Detailed experimental measurements on blood and RBC suspensions revealed a very good correlation between $\sqrt{\tau}$ and $\sqrt{\dot{\gamma}}$ [12]. The yield stress value depends on the RBC concentration (Ht) and concentration C_{fbg} of the protein fibrinogen (fbg) which is responsible for the REB aggregation: $\tau_0 = \tau_0(Ht, C_{fbg})$. A typical value for healthy blood is accepted as $\tau_0 = 0.005 N/m^2$. The most frequently used approximations are

$$\begin{aligned} \sqrt{\tau_0} &= (Ht - 0.07)^{3/2} (0.49C_{fbg} + 0.24); \\ \sqrt{\tau_0} &= 0.01 (Ht - 10) (C_{fbg} + 0.5). \end{aligned} \quad (14)$$

The asymptotic viscosity in blood as a shear-thinning viscoplastic fluid $\mu_\infty = \lim_{\dot{\gamma} \rightarrow \infty} \mu(\dot{\gamma}) = \mu_\infty(Ht, \mu_{bp})$ is also a function of the RBC concentration (Ht) and blood plasma viscosity μ_{bp} . The former is a Newtonian fluid and its viscosity depends on the temperature $\mu_{bp} = \mu_{bp}(T)$ and concentrations C_p of the most important proteins

$$\mu_{bp} = \frac{\mu_0}{1 - k_p C_p}, \quad (15)$$

where $k_p = \text{const}$ determined for the prevalent proteins.

When (14) is used in the rheological model, the resulting system of PDE must be completed by the diffusion equation for C_p .

In 1926 the linear Bingham model (10) was generalized by W. Hershel and R. Bulkeley in the form

$$\tau = \tau_0 + \mu \dot{\gamma}^n, \quad \text{when } \tau > \tau_0. \quad (16)$$

The model (16) gives

- 1) Newtonian fluid at $\tau_0 = 0, \quad n = 1$;
- 2) Shear-thinning fluid at $\tau_0 = 0, \quad 0 < n < 1$;
- 3) Ostwald model (5) at $\tau_0 = 0$;
- 4) Bingham fluid (10) at $\tau_0 > 0, \quad n = 1$;
- 5) Generalized viscoplastic shear-thinning fluid at $\tau_0 > 0, \quad 0 < n < 1$.

The tensorial form of (16) can be written as

$$\tau_{ik} = 2\mu_b(I_{2v})v_{ik}, \quad \mu_b(I_{2v}) = kI_{2v}^{n-1} + \frac{\tau_0}{I_{2v}}, \quad (17)$$

where k is the constant from (5).

The second expression (17) can be reformulated for the 1D flow as

$$u_b(\dot{\gamma}) = \begin{cases} \mu_0, & \text{when } \tau < \tau_0, \\ \tau_0 |\dot{\gamma}|^{-1} + k |\dot{\gamma}|^{-1}, & \text{when } \tau > \tau_0, \end{cases} \quad (18)$$

where $\mu_0 = \tau_0 |\dot{\gamma}_0|^{-1} + k |\dot{\gamma}_0|^{-1}$, $\dot{\gamma}_0$ is the critical shear rate corresponded to the yield shear stress τ_0 .

Substitution (17) into the Navier-Stokes equations gives for the Poiseuille flow between the parallel plates located at the distance H [20]

$$\frac{\partial p}{\partial x} = \frac{\partial}{\partial y} \left(\mu_b \frac{\partial v}{\partial y} \right) = \begin{cases} \mu_b \frac{\partial^2 v}{\partial y^2}, & \text{when } \left| \left(\frac{\partial v}{\partial y} \right) \right| < \gamma_0, \\ \frac{\partial}{\partial y} \left(\left(k \left(\frac{\partial v}{\partial y} \right)^{n-1} + \tau_0 \left(\frac{\partial v}{\partial y} \right)^{-1} \right) \left(\frac{\partial v}{\partial y} \right) \right), & \\ \text{when } \left| \left(\frac{\partial v}{\partial y} \right) \right| \geq \gamma_0. \end{cases} \quad (19)$$

Solution of (19) with the no-slip BC at the plates is

$$v(y) = \begin{cases} \frac{n}{(n+1)\pi_0} \left(((y-\delta)\pi_0 + \dot{\gamma}_0^n)^{\frac{n}{n+1}} - (\dot{\gamma}_0^n - \delta\pi_0)^{\frac{n}{n+1}} \right), & \\ y \in [0, \delta[, \quad \left| \frac{\partial v}{\partial y} \right| > \gamma_0, \\ \frac{\pi_0}{2\mu_0} y(y-1) + k, & y \in [\delta, 1-\delta[, \quad \left| \frac{\partial v}{\partial y} \right| < \gamma_0, \\ \frac{n}{(n+1)\pi_0} \left((\dot{\gamma}_0^n - (y-1+\delta)\pi_0)^{\frac{n}{n+1}} - (\dot{\gamma}_0^n - \delta\pi_0)^{\frac{n}{n+1}} \right), & \\ y \in [1-\delta, 1], \quad \frac{\partial v}{\partial y} < -\gamma_0, \end{cases} \quad (20)$$

where $\pi_0 = -\Delta P \frac{h}{L} \frac{\mu_0 \gamma_0 - \gamma_0^n}{\tau_0}$, $\delta = \frac{\mu_0 \gamma_0}{|\pi_0|}$, k is computed from (19) according to the velocity continuity conditions at the interfaces $y = \delta; 1 - \delta$.

Expression (20) gives flattened shear-rate dependent velocity profiles $v(r^{/circ})$, where $r^{/circ} = 2r/H$ (Fig.4).

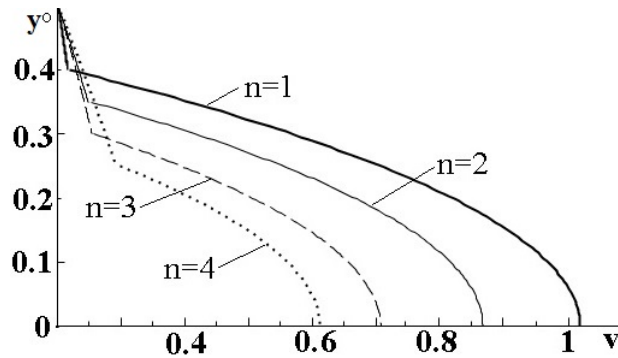


Fig. 4. Velocity profiles for generalized viscoplastic fluid (20) at $n=1,2,3,4$.

Efficient viscosity of the Hershel-Bulkley fluid (17) in steady laminar flow can be written as [22]

$$\mu_{eff} = \mu_0 \left(\frac{8v_{av}}{h} \right)^{n-1} \left(\frac{3n+1}{4n} \right)^n \frac{(1-X)^{-1}}{(1-aX-bX^2-cX^3)^n}, \quad (21)$$

where $X = \frac{4L\tau_0}{h\Delta P}$, $a = (2n+1)^{-1}$, $b = 2na(n+1)^{-1}$, $c = bn$, v_{av} is an averaged velocity of the fluid flow through the channel.

Numerical computations on (20) showed a good correspondence with experimental measurements on different fluids. When the Reynolds number is computed based on the efficient viscosity $Re = \rho v_{av} h \mu_{eff}^{-1}$, the standard Newtonian friction factor

$$f = \frac{64}{Re_{eff}} \quad (22)$$

is in agreement with measurement data.

The Hershel-Bulkley model is used for optimization of the long-range pipelines pumping such non-Newtonian fluids like oil. This model gives good results for steady [23] and pulsatile [24] blood flow through the curved and stenosed arteries.

2.4. Viscoelastic models

Due to viscoelasticity of the erythrocyte membranes, their aqueous suspensions possess complex viscoelastic properties with stress and strain relaxations after each cycle of load-discharge by the external forces. The simplest 3-element model of blood as a suspension of the fluid-filled elastic shells is the Jeffrey model [25]

$$k_1 \frac{\partial \tau_{ik}}{\partial t} + \tau_{ik} = \mu_{bp} \frac{\partial v_{ik}}{\partial t} + k_2 \frac{\partial^2 v_{ik}}{\partial t^2}, \quad (23)$$

where $k_1 = (\mu_{Hb} + \mu_{bp})/E_m$, $k_2 = \mu_{Hb}\mu_{bp}/E_m$, E_m is the Young modulus of the membrane, μ_{Hb} and μ_{bp} are the viscosities of the hemoglobin solutions inside the erythrocytes and the blood plasma.

More sophisticated models accounted for the membrane sublayers and viscoelasticity of the blood plasma can be written in the general form

$$\dots + k_3 \frac{\partial^2 \tau_{ik}}{\partial t^2} + k_1 \frac{\partial \tau_{ik}}{\partial t} + \tau_{ik} = \mu_0 v_{ik} + k_2 \frac{\partial v_{ik}}{\partial t} + k_4 \frac{\partial^2 v_{ik}}{\partial t^2} + \dots \quad (24)$$

3. Mathematical problem formulations for generalized rheological laws

Substitution (24) into the Navier-Stokes equations gives the momentum equation (linearized 1D case) in the form

$$\left[\dots + k_3 \frac{\partial^2}{\partial t^2} + k_1 \frac{\partial}{\partial t} + I \right] \left(\rho \frac{\partial v}{\partial t} + \frac{\partial p}{\partial x} \right) = \left[\mu_0 I + k_2 \frac{\partial}{\partial t} + k_4 \frac{\partial^2}{\partial t^2} + \dots \right] \frac{\partial^2 v}{\partial x^2}, \quad (25)$$

where I is the unit operator.

When $k_{1-4} = 0$, (25) gives the 1D equation for Newtonian fluids. When $k_{2-4} = 0$, $k_1 \neq 0$, the hyperbolic equation (25) describes the wave propagation in the viscoelastic fluid. In the case of plane waves propagation through a long fluid-filled soft tube with a given unstrained cross-section profile $S_0(x)$, the well-known J.Lighthill's model can be generalized for the viscoelastic fluid with rheological equation (24) in the form

$$\begin{cases} \frac{\partial S}{\partial t} + S_0 \frac{\partial U}{\partial x} = 0, \\ \frac{\partial U}{\partial t} + \frac{1}{\rho} \frac{\partial P}{\partial x} - \frac{\mu_0 U}{S_0} = 0, \\ \dots + k_4 \frac{\partial^2 S}{\partial t^2} + k_2 \frac{\partial S}{\partial t} + S = k_0 P + k_1 \frac{\partial P}{\partial t} + k_3 \frac{\partial^2 P}{\partial t^2} + \dots, \end{cases} \quad (26)$$

where P and U are the mean pressure and flow velocity through the cross-section of the tube, k_0^{-1} is the circumferential elasticity of the soft tube per unit length.

By excluding the variables $S(t, x)$ and $P(t, x)$ from (26), one can obtain a partial derivative differential equation for $U(t, x)$ in the form

$$\begin{aligned} \dots - k_3 \frac{\partial^4 U}{\partial t^4} + \left(\frac{k_3 \mu_0}{S_0} - k_1 \right) \frac{\partial^3 U}{\partial t^3} + \left(\frac{k_1 \mu_0}{S_0} - k_0 \right) \frac{\partial^2 U}{\partial t^2} + \frac{k_0 \mu_0}{S_0} \frac{\partial U}{\partial t} + \\ \frac{S_0}{\rho} \frac{\partial^2 U}{\partial x^2} + \frac{k_2 S_0}{\rho} \frac{\partial^3 U}{\partial t \partial x^2} + \frac{k_4 S_0}{\rho} \frac{\partial^4 U}{\partial t^2 \partial x^2} + \dots = 0. \end{aligned} \quad (27)$$

Eq.(27) has a solution in the form of running wave $U(t, x) = U^* \cdot \exp(i(\omega t - nx))$, where U^* is the amplitude, n is the wave number. Substitution gives the dispersion equation

$$\dots + \omega^4 + ip_1 \omega^3 + \omega^2 (p_2 - p_3 n^2) + i\omega (p_4 n^2 - p_5) + p_6 n^2 = 0, \quad (28)$$

where $p_1 = \frac{\mu_0}{S_0} - \frac{k_1}{k_3}$, $p_2 = \frac{k_1 \mu_0}{k_3 S_0} - \frac{k_0}{k_3}$, $p_3 = \frac{k_4 S_0}{k_3 \rho}$, $p_4 = \frac{k_2 S_0}{k_3 \rho}$, $p_5 = \frac{k_0 \mu_0}{k_3 S_0}$, $p_6 = \frac{S_0}{k_3 \rho}$.

For the case $k_{5,6,7,\dots} = 0$ the expressions for the wave speed $c(\omega)$ and wave dispersion $\omega(n)$ have been computed in [26]. Numerical computations on the generalized Lighthill-Shapiro model have been performed with the material parameters of blood and arterial vessel walls. Despite the four different solutions for the wave speed obtained in [25] (two Young's fluid-based modes and two Lamb's solid-based modes), the model (28) gives more types of the solid-based wave modes which could characterize the micro- and nanostructure of the wall material. The models with additional relaxation times gives the stress-strain rate curves, strain relaxation curves in the isotopic experiments and stress relaxation curves in the isometric experiments which fit better to the experimental curves

measured on biological tissues compared to the standard 3-element rheological models [27].

In the 3D case (24) can be rewritten as

$$\begin{aligned} & \rho \left(\dots + k_3 \frac{\partial^3 \vec{v}}{\partial t^3} + k_1 \frac{\partial^2 \vec{v}}{\partial t^2} + \frac{\partial \vec{v}}{\partial t} \right) = \\ & = - \left[I + k_1 \frac{\partial}{\partial t} + k_3 \frac{\partial^2}{\partial t^2} + k_5 \frac{\partial^3}{\partial t^3} + \dots \right] \nabla p + \\ & + \left[\mu_0 + k_2 \frac{\partial}{\partial t} + k_4 \frac{\partial^2}{\partial t^2} + k_6 \frac{\partial^3}{\partial t^3} + \dots \right] \Delta \vec{v}. \end{aligned} \quad (29)$$

Eq.(29) also admits wave solutions in the form of normal mode

$$f(t, x) = f^* \cdot \exp(i(\omega t - n\vec{r})), \quad f = \{p, \vec{v}\}. \quad (30)$$

Substitution of (30) into (29) gives the sound speed and dispersion in the bulk viscoelastic fluid. In the case of a long axisymmetric fluid-filled distensible tubes when the fluid flow is initiated by periodic pressure oscillations $P(t)|_{x=0} = P^* e^{i\omega t}$ at the inlet of the tube, (30) describes 2D cylindrical wave propagation $v_x(t, r, x) = v^*(r) \cdot \exp(i\omega(t - x/c))$, $c = \omega/n(\omega)$, and the wave amplitude is a solution of the Bessel's equation

$$\frac{1}{r} \frac{\partial}{\partial r} \left(r \frac{\partial v^*}{\partial r} \right) - \Xi v^*(r) = \Theta P^*, \quad (31)$$

$$\begin{aligned} \text{where } \Xi &= \rho \frac{\dots - ik_3\omega^3 - k_1\omega^2 + i\omega}{\mu_0 + ik_2\omega - k_4\omega^2 - ik_6\omega^3 + \dots} + \frac{\omega^2}{c^2}, \\ \Theta &= \frac{i\omega(1 + ik_1\omega - k_3\omega^2 - k_5\omega^3 + \dots)}{c(\mu_0 + ik_2\omega - k_4\omega^2 - ik_6\omega^3 + \dots)}. \end{aligned}$$

In the case $k_{5,6,7,\dots} = 0$ the solution of (31) has been computed and analyzed in [28] for the material parameters corresponded to blood as the fluid and arterial vessel wall of healthy individuals and patients with some diseases.

Similar problem formulations can be derived for shear-thinning and viscoplastic models as well as their combinations with viscoelastic model (25). For each separate case the problem of solution existence and uniqueness, stability and physical relevance must be studied. Moreover, correct formulation of boundary and initial conditions for the partial differential equations with time derivatives of order $n \geq 2$ must be a case for special considerations.

4. Conclusions

Real liquids usually possess more complex rheological properties that cannot be described by uniform Newtonian fluids. Many sophisticated constitutive equations for complex solids and fluids have been developed in theoretical rheology. Recently, an attention was attracted by the suspensions of micro- and nanoparticles (micro/nanofluids, respectively), and blood is one the most studied microfluids. The rheological models developed for blood and other suspensions can be divi-

ded into the shear-thinning, viscoplastic, viscoelastic general models. Their combinations allow characterization of their viscous, elastic, shear rate dependent, yield stress (tixotropy) and other mechanical properties. Substitution of more general rheological laws into the Navier-Stokes equations for viscous fluids give systems of partial differential equations with time derivatives of the orders $n \geq 2$ that needs correct formulations of additional boundary and initial conditions for the variables. It is shown, for the viscoelastic models the governing system of equations is hyperbolic and allows solution in the form of running pressure and flow waves. Due to the high order derivatives, the dispersion relations produce a big variety of the frequency-dependent properties and types of the stress and strain relaxation. Bifurcations and stability of the solutions as well as the problem formulations of the mixed shear-thinning, viscoplastic and viscoelastic rheological properties will be a subject for our future studies.

REFERENCES

1. J. Carson, R. Van Loon, P. Nithiarasu. Mathematical Techniques for Circulatory Systems, Encyclopedia of Biomedical Engineering, Elsevier. – 2019. – P. 79-94. 10.1016/B978-0-12-801238-3.99982-3
2. S.K. Zhou, D. Rueckert, G. Fichtinger. Handbook of Medical Image Computing and Computer Assisted Intervention, Elsevier. – 2020. 10.1016/C2017-0-04608-6
3. W.W. Nichols, M.F. O'Rourke, Ch. Vlachopoulos. McDonald's Blood Flow in Arteries: Theoretical, Experimental and Clinical Principles. CRC Press. – 2011. 10.1201/b13568
4. D. Rubenstein, W. Yin, M. Frame. Biofluid Mechanics. An Introduction to Fluid Mechanics, Macrocirculation, and Microcirculation. Academic Press 2021. 10.1016/C2018-0-02144-1
5. J.R. Womersley. Method for the calculation of velocity, rate of flow and viscous drag in arteries when the pressure gradient is known, J. Physiol. – 1955. Vol. **127**, No **3**. – P. 553-563. 10.1113/jphysiol.1955.sp005276
6. Y.C. Fung. Biomechanics Motion, flow, stress and growth. Springer-Verlag. – 1990. 10.1007/978-1-4757-2257-4
7. F.M. White. Fluid Mechanics. 9-th edition. McGraw Hill. – 2021. M9781260258318
8. P.R. Fahraeus, T. Lindqvist. The viscosity of the blood in narrow capillary tubes, American J. Physiol. – 1931. Vol. **96**. – P. 562–568. 10.1152/ajplegacy.1931.96.3.562
9. N. Kizilova, V. Cherevko. Mathematical modeling of particle aggregation and sedimentation in concentrated suspensions, Mechanika w Medycynie. Rzeszow Univ.Press. – 2014. Vol.**12**. – P.43–52.

10. L. V. Batyuk, N.N. Kizilova. Modeling of laminar flows of the erythrocyte suspensions as Bingham fluids, Bull. T.Shevchenko Kyiv National University. Ser. Physical and Mathematical Sciences. – 2017. No **4**. – P.23–28.
11. V. Cherevko, N. Kizilova. Complex flows of immiscible microfluids and nanofluids with velocity slip boundary conditions, Nanophysics, Nanomaterials, Interface Studies, and Applications, Springer Proceedings in Physics. – 2017. Vol. **183**. P. 207–230. 10.1007/978-3-319-56422-7-15
12. H. Liu, L. Lan, J. Abrigo, et al. Comparison of Newtonian and Non-newtonian Fluid Models in Blood Flow Simulation in Patients With Intracranial Arterial Stenosis, Front. Physiol., Sec. Computational Physiology and Medicine. – 2021. Vol. **12**. 10.3389/fphys.2021.718540
13. N. Elie, S. Sarah, R. Marc, et al. Blood Rheology: Key Parameters, Impact on Blood Flow, Role in Sickle Cell Disease and Effects of Exercise Frontiers in Physiology. – 2019. Vol. **10**. 10.3389/fphys.2019.01329
14. G. Barshtein, A. Gural, O. Zelig, et al. Unit-to-unit variability in the deformability of red blood cells, Transfusion and Apheresis Sci. – 2020. Vol. **59**, No **5**. – P.102876. 10.1016/j.transci.2020.102876
15. Kizilova N.M., Solovjova O.M. Analysis of discrete rheological models of bioactive soft and liquid materials, Visnyk of V.N. Karazin Kharkin National University. Ser. Mathematical modeling. Information Technology. Automated control systems. – 2017. Vol.**35**. – P.21–30.
16. N. Kizilova. Electromagnetic Properties of Blood and Its Interaction with Electromagnetic Fields, Advances in Medicine and Biology. – 2019. Vol. **137**. – P.1–74.
17. V.L. Sigal. The Copley-Scott Blair phenomenon. Will it be explained by the effect of an electric double layer? Biorheology. – 1984. Vol. **21**, No **3**. – P. 297–302. 10.3233/bir-1984-21301 10.3233/bir-1984-21301
18. S. Oka. Copley-Scott Blair phenomenon and electric double layer, Biorheology. – 1984. Vol. **21**, No **3**. – P. 417–421. 10.3233/bir-1984-21311
19. A. Yazdani, Y. Deng, H. Li, et al. Integrating blood cell mechanics, platelet adhesive dynamics and coagulation cascade for modelling thrombus formation in normal and diabetic blood, J. Royal Soc. Interface. – 2021. Vol. **18**, No**175**. – P. 33530862. 10.1098/rsif.2020.0834
20. D.J. Acheson. Elementary Fluid Mechanics. Oxford Applied Mathematics and Computing Science Series. – 1990. 10.1002/aic.690380518
21. N.S. Wahid, N.M. Arifin, M. Turkyilmazoglu, et al. Effect of magnetohydrodynamic Casson fluid flow and heat transfer past a stretching surface in porous medium with slip condition, J. Physics: Conference Series. – 2019. Vol. 1366. – P. 012028. 10.1088/1742-6596/1366/1/012028
22. A.K.T. Radhakrishnan, C. Poelma, J. van Lier, F. Clemens. Laminar-turbulent transition of a non-Newtonian fluid flow, J. Hydraulic Res. – 2021. Vol. **59**, No. **2**. – P. 235-249. 10.1080/00221686.2020.1770876

23. N. A. Konan, E. Rosenbaum, M. Massoudi. On the response of a Herschel-Bulkley fluid due to a moving plate, *Polymers*. – 2022. Vol. 14. – P.3890. 10.3390/polym14183890
24. Z. Abbas, M. S. Shabbir. Analysis of rheological properties of Herschel-Bulkley fluid for pulsating flow of blood in π -shaped stenosed artery, *AIP Advances*. – 2017. Vol. 7, No 10. – P. 105123. 10.1063/1.5004759
25. M. Asgir, A. A. Zafar, A. M. Alsharif, et al. Special function form exact solutions for Jeffery fluid: an application of power law kernel, *Adv. Differ. Equ.* – 2021. Vol. 384. – P.2021. 10.1186/s13662-021-03539-x
26. N. M. Kizilova, I. V. Mayko. Generalization of the Lighthill's problem for the case of tubes with complicated wall rheology filled with a viscous liquid, *Bull. T.Shevchenko Kyiv National University. Ser. Physical and Mathematical Sciences*. – 2020. No 1-2. – P.67–70.
27. N. M. Kizilova, O. M. Solovjova. Analysis of discrete rheological models of bioactive soft and liquid materials. *Visnyk of V.N. Karazin Kharkiv National University. Ser. Mathematical modeling. Information Technology. Automated control systems*. – 2017. Vol. 35. – P.21–30.
28. Ya. I. Braude, N. M. Kizilova Study on periodic axisymmetric flow of viscoelastic fluid through a cylindrical tube. *Bull. T.Shevchenko Kyiv National University. Ser. Physical and Mathematical Sciences*. – 2020. No 1-2. – P.49–52.

Article history: Received: 4 January 2023; Final form: 17 May 2023

Accepted: 7 June 2023.

How to cite this article:

L. V. Batyuk, N. M. Kizilova, S. O. Poslavsky, A review on rheological models and mathematical problem formulations for blood flows, *Visnyk of V. N. Karazin Kharkiv National University. Ser. Mathematics, Applied Mathematics and Mechanics*, Vol. 97, 2023, p. 25–40. DOI: 10.26565/2221-5646-2023-97-03

Огляд реологічних моделей і постановок математичних задач для кровотоку

Батюк Л. В.¹, Кізілова Н. М.², Пославський С. О.²

¹ Харківський національний медичний університет
проспект Науки 4, 61000, Харків, Україна

² Харківський національний університет імені В. Н. Каразіна
майдан Свободи 4, 61022, Харків, Україна

Наведено огляд реологічних рівнянь, які запропоновані в літературі для математичного моделювання ламінарних і турбулентних течій крові як концентрованої суспензії м'яких частинок. Детально обговорюються реологічні моделі крові як однорідної ньютонівської та неньютонівської рідин; рідини, що розріджують зі зсувом; в'язкопластичної; в'язкопружної; тиксотропної та мікрморфної рідин. Згідно з наведеними експериментальними даними, адекватна реологічна модель крові повинна

описувати псевдопластичну і тіксотропну поведінку з залежними від концентрації в'язкопружними властивостями, які властиві крові здорової людини. Ці властивості можна детальніше вивчати на відповідних математичних формулюваннях задач для течій крові крізь трубки або канали. Обговорені системи рівнянь і граничні умови для кожної із запропонованих реологічних моделей. Точні рішення для стаціонарних ламінарних течій між паралельними пластинами та через трубки кругового перерізу виписані та проаналізовані для рідин Оствальда, Гершеля-Балклі та Бінгама. Для кожної моделі досліджено вплив параметрів моделі на профілі швидкості. Показано, що певні набори параметрів рідини призводять до сплюснення профілю швидкості, а інші викликають його загострення навколо осі каналу. Показано, що члени другого порядку в моделях в'язкопружності приводять до систем диференціальних рівнянь з частинними похідними з високими порядками за часом і змішаними просторово-часовими похідними. Наведені відповідні постановки задач для хвильових течій рідин з узагальненими реологічними законами крізь м'які трубки. Отримано аналітичні розв'язки для швидкості течії, гідростатичного тиску і площі перерізу трубки у вигляді нормальних мод. Показано, що дисперсійні рівняння дають додатковий набір для швидкості звуку (так званий другий звук) у рідині. Зроблено висновок, що найбільш загальна реологічна модель повинна включати ефекти псевдопластичні, концентрації частинок та другого звуку.

Ключові слова: диференціальні рівняння; реологічні моделі; суспензії; гідродинаміка.

Історія статті: отримана: 4 січня 2023; останній варіант: 17 травня 2023
прийнята: 7 червня 2023.